Deactivation and regeneration of ruthenium on silica in the liquid-phase hydrogenation of butan-2-one

Haresh G. Manyar [a], Daniel Weber [b], Helen Daly [a], Jillian M. Thompson [a], David W. Rooney [a], Lynn F. Gladden [b], E. Hugh Stitt [c], J. Jose Delgado [d], Serafin Bernal [d], Christopher Hardacre [a,*]

[a] CenTACat, School of Chemistry and Chemical Engineering, Queen's University Belfast, David Keir Building, Stranmillis Road, Belfast BT9 5AG, UK
[b] Dept. of Chemical Engineering and Biotechnology, University of Cambridge, Pembroke St., Cambridge CB2 3RA, UK
[c] Johnson Matthey Catalysts, P.O. Box 1, Belasis Avenue, Billingham TS23 1LB, UK
[d] Departamento de Ciencia de los Materiales e Ingeniería Metalúrgica y Química Inorgánica, Facultad de Ciencias, Universidad de Cádiz, Campus Río San Pedro, E-11510 Puerto Real (Cádiz), Spain

ARTICLE INFO

ABSTRACT

A Ru/SiO$_2$ catalyst was investigated for the liquid-phase hydrogenation of butan-2-one to butan-2-ol with water as a medium. Although excellent reactivity was observed, a gradual deactivation of the catalyst was found on recycle of the catalyst. The spent catalyst was characterized by using XRD, XPS, TEM, TPR, CO chemisorption, FTIR and ICP analyses. Formation of Ru(OH)$_x$ surface species is proposed to be the main cause of catalyst deactivation with no significant Ru leaching into the reaction mixture. Following catalyst regeneration, up to 85% of the initial catalytic activity could be recovered successfully. Moreover, adsorption of secondary aliphatic alcohols on the catalyst was found to significantly reduce the formation of Ru(OH)$_x$ during the reaction, thus protecting the catalyst from deactivation.

© 2009 Elsevier Inc. All rights reserved.

1. Introduction

Noble metal-based catalysts are commonly used to perform a range of hydrogenations for the production of bulk, fine and pharmaceutical chemicals. However, there is a major concern about the deactivation of the catalyst, in particular for large-scale processes where the capital cost of the catalyst is high. The loss of catalyst activity and selectivity, which is, in general, due to structural and morphological changes of the active sites on the catalyst surface, has a significant effect on the impact of such catalysis in various processes of high industrial importance [1–4]. Although catalyst deactivation mechanisms have been examined extensively, the majority of studies have been limited to gas-phase reactions with only limited studies concerning catalyst deactivation in liquid-phase hydrogenations [5]. The main causes of the catalyst deactivation in the liquid-phase were found to be phase transformations of active components (sintering or leaching); coking; poisoning of the active site by heteroatom-containing molecules, impurities in solvents and reagents or oligomeric and polymeric by-products or by deposition of an overlayer of less active or totally inactive metal or metal oxide on noble metal surface [6–9].

Although platinum group metals (PGMs) are widely used catalysts in hydrogenations, the utilization of ruthenium catalysts has only been reported for specific reactions, for example in the hydrogenation of carboxylic acids [10,11]. Herein, ruthenium is used to hydrogenate butan-2-one to the corresponding alcohol. In this respect, for the reduction of aliphatic carbonyl compounds, ruthenium-based catalysts have been demonstrated to show high activity in particular in the presence of water [12]. The enhancement in the catalytic activity has been attributed to a number of different factors. It has been suggested that the catalytically active species is a hydrate of ruthenium formed by a water and ruthenium complex [13–15]. Alternatively, density functional theory calculations have shown that small amounts of water can enhance the hydrogenation activity of metal catalysts by providing a low energy route for hydrogen activation. This occurs via a proton shuttle mechanism through strong hydrogen bonding of the solvent at the catalyst surface [16]. Reactions in a water/propan-2-ol mixed solvent system have also recently been investigated by Hu et al. for the catalytic hydrogenation of 2-butyne-1,4-diol [17]. In this case, a complex trend of reaction rate as a function of the ratio of water and propan-2-ol used was observed, which could be rationalized using a combination of changes in hydrogen solubility and the average gas bubble size formed in the solvent mixture. Recently, we have investigated the role of water in a mixed solvent

---

* Corresponding author. Fax: +44 28 90 974687.
E-mail address: c.hardacre@qub.ac.uk (C. Hardacre).

system for the hydrogenation of butan-2-one over a Ru/SiO$_2$ catalyst using a combination of experimental and theoretical data to study the effect of the solvent composition on mass transfer, diffusion and reaction kinetics and mechanism [18]. This paper reports further insight into the fate of the active ruthenium species on the catalyst surface by the detailed investigation of the deactivation of the ruthenium on silica catalyst in butan-2-one hydrogenation. To the best of our knowledge, there are no reports on the deactivation of ruthenium due to hydration of ruthenium catalysts to ruthenium hydroxide in water. In addition, the effect of the addition of a range of alcohols to the solvent medium was studied with respect to the deactivation of the catalyst during reaction.

2. Experimental

2.1. Chemicals and catalyst

All the chemicals were of AR grade from Sigma–Aldrich and were used without further purification. All gases used were of BOC research grade. Ruthenium (III) chloride hydrate was obtained from Aldrich.

1 wt% Ru/SiO$_2$ (average particle size 20–45 μm) was prepared by an incipient wetness technique using aqueous ruthenium (III) chloride trihydrate solution. The catalyst was dried at 120 °C in air, followed by reduction in 5% H$_2$ in He at 400 °C for 3 h.

Ru(OH)$_3$ was prepared by precipitation from a solution of RuCl$_3 \cdot x$H$_2$O (65.1 mg), dissolved in 30 cm^3 of distilled deionised water. The pH of the solution was adjusted to 13.2 by addition of an aqueous solution of NaOH (1 M) and the resulting slurry was stirred for 24 h at room temperature. The solution was filtered and the solid was washed with copious amounts of water. The product was dried at 105 °C in a flow of argon to obtain Ru(OH)$_3$ as a dark green powder.

2.2. Catalyst characterization

X-ray diffraction measurements were made with Cu K$_\alpha$ radiation (1.5405 Å) on a PANalytical X'PERT PRO MPD diffractometer equipped with reflection geometry, a NaI scintillation counter, a curved graphite crystal monochromator and a nickel filter. The scattered intensities were collected from 5° to 80° (2θ) by scanning at 0.017° (2θ) steps with a counting time of 0.5 s at each step.

The surface area, total pore volume and average pore diameter were measured by N$_2$ adsorption-desorption isotherms at 77 K using Micromeritics ASAP 2010. The pore size was calculated on the adsorption branch of the isotherms using Barrett–Joyner–Helenda (BJH) method and the surface area was calculated using the Brunauer–Emmett–Teller (BET) method.

Quantification of the silanol groups on the surface of catalyst was performed by liquid-phase silylation with trimethylethoxysilane (TMES), following the procedure outlined by Hruby and Shanks, [19] followed by measurement of the total organic carbon (TOC) content of the silylated samples to calculate the surface coverage silanol groups as reported by Sever et al. [20]. Liquid-phase silylations were performed by adding TMES (2 cm^3) to a suspension of SiO$_2$ or 1 wt% Ru/SiO$_2$ catalyst (500 mg) in toluene (20 cm^3) under vigourous stirring at 90 °C for 2 h under a N$_2$ atmosphere. The mixture was filtered, and the silylated samples were washed several times with toluene and dried in air at 115 °C for 10 h.

Temperature-programmed reduction (TPR) was measured using approximately 0.1 g of fresh catalyst in a Micromeritics Autochem 2910. The samples were placed in a U-shaped tube and cooled to −50 °C in argon. The catalyst was reduced using 5% H$_2$ in Ar with the temperature being ramped from 20 to 800 °C at a rate of 5 °C min^{-1}. Hydrogen uptake, as monitored by a thermal conductivity detector (TCD), was recorded.

CO chemisorption measurements were made using a Micromeritics Autochem 2910 to monitor CO uptake while pulsing CO over the catalyst at 4 °C. Approximately 0.1 g of catalyst was prereduced in 5% H$_2$ in Ar for 240 min at the desired temperature, then purged with He for 60 min before cooling to 4 °C. A mixture of 10% CO in He was pulsed into the reactor every 5 min, and the uptake as measured by the TCD was recorded until the catalyst was saturated.

The XPS spectra were obtained using a Kratos AXIS Ultra DLD XPS spectrometer using monochromated Al K$_\alpha$ X-rays and a hemispherical analyser with a pass energy of 160 eV. The powdered samples were mounted on conducting copper tape and the binding energies were normalized to the C 1 s at 284.6 eV. Background subtraction was performed using a Shirley background [21] and CasaXPS.

Metal analysis was performed using a Perkin–Elmer Optima 4300 ICP-OES to check for the leaching of ruthenium in the reaction filtrate. The reaction mixture was filtered to remove catalyst particles, the solvent evaporated and the residue dissolved in concentrated nitric acid.

Infrared spectroscopy was used to investigate the adsorption of alcohols on the catalyst as well as the relative rates at which water, butan-2-one, propan-1-ol and propan-2-ol displace each other from a Ru/SiO$_2$ surface. FTIR spectra of the catalysts following the adsorption of alcohols on the fresh catalyst were recorded at room temperature in a Bruker TENSOR 27 spectrometer in the range 4000–400 cm^{-1}, with a resolution of 4 cm^{-1} using 64 scans. For the rates of displacement study, 1 wt% Ru/SiO$_2$ was reduced at 400 °C under flowing H$_2$ at 40 cm^3 min^{-1} prior to adsorption of propan-1-ol, propan-2-ol or water at 75 °C. Liquid butan-2-one, propan-1-ol, propan-2-ol and water were delivered to the DRIFTS cell by entrainment in a flow of Ar at 20 cm^3 min^{-1}. Spectra were recorded using a Bruker Equinox 55 spectrometer, with an average of 30 scans at 4 cm^{-1}. Following adsorption of water, the feed was switched to either propan-1-ol or propan-2-ol with spectra recorded every 15 s. The intensity of the bands in the 2800–3000 cm^{-1} region due to CH$_3$/CH$_2$ stretching vibrations of propan-1-ol and propan-2-ol was monitored to evaluate the rate at which propan-1-ol or propan-2-ol can displace water and adsorb on the Ru/SiO$_2$ surface. The same experiment was carried out with initial adsorption of propan-1-ol or propan-2-ol before switching the feed to water to evaluate the ability of water to displace adsorbed propan-1-ol and propan-2-ol. In addition, the effect of propan-2-ol adsorption on the rate of butan-2-one adsorption was studied, in this case the C–H stretching frequency in the region 2850–3000 cm^{-1} was monitored.

The transmission electron microscopy (TEM) studies were performed on a JEOL 2010-FEG instrument, at 100 kV. Ruthenium particle size distributions were obtained by operating the microscope in the scanning-transmission electron microscopy (STEM) mode, with the help of a HAADF (High Angle Annular Dark Field) detector. This approach has shown to be particularly useful to obtain reliable size distribution data in supported metal catalysts. The high resolution nano-analytical studies were carried out by using a X-EDS detector (Oxford Instruments) and an electron probe with a diameter as small as 0.7 nm. The sample powders were directly deposited without solvent on a holey carbon film supported on 3 mm grid. No solvents were used in this sample deposition routine.

2.3. Hydrogenation procedure

All experiments were carried out in a 100 cm^3 Hazard Evaluation Laboratory (HEL) AutoMATE pressure reactor equipped with a gas-inducing impeller with online hydrogen consumption monitoring. The solvents used were distilled, deionised, >18 MΩ ultra-

pure water and/or alcohol. The alcohols used were propan-2-ol, butan-2-ol, propan-1-ol, ethanol and methanol. Typically, the reactor was charged with solvent (17 cm^3), 1 wt% Ru/SiO$_2$ catalyst (60 mg, pre-reduced and dehydrated at 400 °C for 4 h in a flow of H$_2$) and butan-2-one (2.2 g, 30.5 mmol). After purging with N$_2$, the solvent was heated to the desired temperature (60 °C) and hydrogen was introduced. After purging with H$_2$, the reactor was pressurized to 4 bar and the stirring started. The kinetics of the reaction were monitored by hydrogen consumption using a Brooks mass flow controller. In addition, liquid samples (~1 cm^3) were analyzed using a GC equipped with a DB-1 capillary column and FID detector.

The reusability of 1 wt% Ru/SiO$_2$ catalyst was studied by recovering the catalyst by filtration at the end of the butan-2-one hydrogenation under typical experimental conditions as mentioned above. The recovered catalyst was washed with ultrapure water and reused as before. To test for deactivation due to oxidation by air, butan-2-one (2.2 g) hydrogenation was performed under typical experimental conditions using fresh 1 wt% Ru/SiO$_2$ catalyst (60 mg, pre-reduced at 400 °C for 4 h in a flow of H$_2$) until completion. Thereafter, fresh butan-2-one (2.2 g) was added without removal of the catalyst and the reaction restarted. This procedure was repeated up to 6 consecutive runs.

To study the deactivation kinetics, the influence of the time spent by the catalyst in water was investigated. Separate hydration experiments were carried out by stirring 1 wt% Ru/SiO$_2$ catalyst (60 mg, pre-reduced at 400 °C for 4 h in a flow of H$_2$) in 17 cm^3 of ultrapure water under 4 bar H$_2$ pressure at 60 °C for 0, 2, 4 and 6 h before the addition of butan-2-one (2.2 g). The hydrogenation activity of 1 wt% Ru/SiO$_2$ catalyst (hydrated for 0–6 h) was followed by monitoring the H$_2$ uptake in the reaction.

The effect of alcohol addition to the solvent was examined by pretreating the reduced catalyst in 17 cm^3 of ultrapure water under 4 bar H$_2$ pressure at 60 °C for 2 h in the presence of 30.5 mmol of a range of primary and secondary alcohols. The quantity of alcohol (30.5 mmol) was chosen since it was the stoichiometric equivalent of butan-2-one. The effect of the concentration of alcohol was examined over the range 0.44–2.61 M, i.e. 0.25–1.50 molar equivalents using butan-1-ol. A separate experiment was carried out to check for the influence of a pure layer of butan-2-ol on the catalyst surface. The catalyst was washed with butan-2-ol and the excess alcohol was removed, thereby leaving behind a coated layer on the catalyst particles. Hydration of the butan-2-ol-coated catalyst was performed under similar experimental conditions and it was subsequently checked for the hydrogenation activity.

For catalyst regeneration experiments, completely deactivated 1 wt% Ru/SiO$_2$ catalyst, obtained by hydrating the catalyst for 6 h, was pre-reduced at temperatures between 400 and 600 °C in a flow of H$_2$ for 4 h and the hydrogenation activity was measured.

3. Results and discussion

3.1. Hydrogenation of butan-2-one

Butan-2-one hydrogenation was carried out in water as a solvent using 1 wt% Ru/SiO$_2$ under experimental conditions previously optimized so that the reaction was performed in the intrinsic kinetic regime, where mass transfer limitations were negligible. For optimization of the reaction conditions, the speed of agitation was varied from 400 to 1400 rpm. There was a significant increase in the initial rate of reaction and butan-2-one conversion on going from 400 to 1200 rpm, but it was almost constant beyond 1200 rpm. This indicated that the gas to liquid mass transfer limitation was absent beyond 1200 rpm. All further reactions were carried out at 1400 rpm. The effect of particle size on the initial rate of reaction and overall conversion of butan-2-one was studied in the range of 20–250 μm. A small increase in the initial reaction rate was observed, when the catalyst particle size was decreased from 250 to 150 and then to 53 μm. There was no appreciable change in the initial rate of reaction and butan-2-one conversion, when the particle size was further decreased beyond 53–20 μm. This study suggests that below a particle size of 53 μm there was no appreciable resistance to intraparticle diffusion. Similarly, liquid to solid mass transfer, which is also a function of particle size, was thus considered as negligible. All further reactions were carried out using a catalyst particle size in the range of 20–45 μm.

3.2. Reusability of 1 wt% Ru/SiO$_2$ catalyst

The reusability of 1 wt% Ru/SiO$_2$ catalyst was examined by using a recovered catalyst at the end of the hydrogenation of butan-2-one under typical experimental conditions. The recovered and washed 1 wt% Ru/SiO$_2$ catalyst showed a significant loss in hydrogenation activity. A further loss in activity was observed on recycling the catalyst for a second time as shown in Fig. 1. This deactivation was attributed to the fast oxidation of Ru to RuO$_2$ on the catalyst surface due to exposure of the catalyst. Hence, a modified recycle methodology was used to study the hydrogenation activity of the 1 wt% Ru/SiO$_2$ catalyst. Here, after the initial reaction was complete, a fixed quantity of 2-butanone was added to the reaction mixture and reaction was continued under same
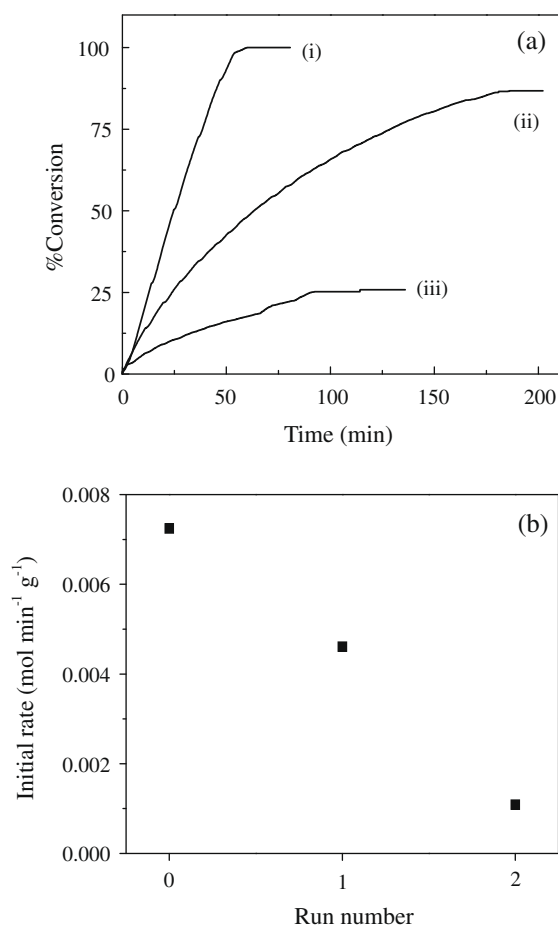

Fig. 1. (a) Butan-2-one conversion with respect to time for (i) the initial reaction, (ii) the first and (iii) the second recycle of the catalyst and (b) the initial hydrogenation rate for the corresponding reactions. In each case, the catalyst was filtered, washed and reused.

experimental conditions until completion. This experiment was repeated to give 6 consecutive runs with the results shown in Fig. 2. Although the catalyst showed good reusability with complete conversion of 2-butanone in each subsequent reaction, the initial rates of hydrogenation decreased linearly with each sequential run. ICP analysis of the filtrate following reaction showed no significant leaching of ruthenium, irrespective of the conditions used.

The deactivation was found to be reversible to some extent. A completely deactivated catalyst was prepared by treating the fresh 1 wt% Ru/SiO$_2$ catalyst in water for 6 h at 60 °C under 4 bar H$_2$ pressure. This catalyst was regenerated by reduction using H$_2$ between 400 and 600 °C for 4 h, and the subsequent hydrogenation activity profiles are shown in Fig. 3. The catalyst regenerated at 500 °C showed higher catalytic activity in comparison with the catalyst regenerated at 400 °C. Further increases in regeneration temperature led to a reduction in the activity of the catalyst. Importantly, at temperatures above 700 °C, the catalyst became inactive.

3.3. Characterization of 1 wt% Ru/SiO$_2$ catalyst

Characterization of the catalyst before and after reaction and after deactivation was performed using XRD, TPR and XPS to examine the state of the catalyst as a result of the reaction.

XRD analysis was performed on the fresh, deactivated (hydrated for 6 h) and regenerated (pre-reduction in H$_2$ at 500 °C) samples of 1 wt% Ru/SiO$_2$ catalyst and the XRD patterns obtained were compared with the XRD pattern of the SiO$_2$ support used in the preparation of 1 wt% Ru/SiO$_2$ catalyst. No peaks other than those from the silica support were observed in the XRD patterns of any of
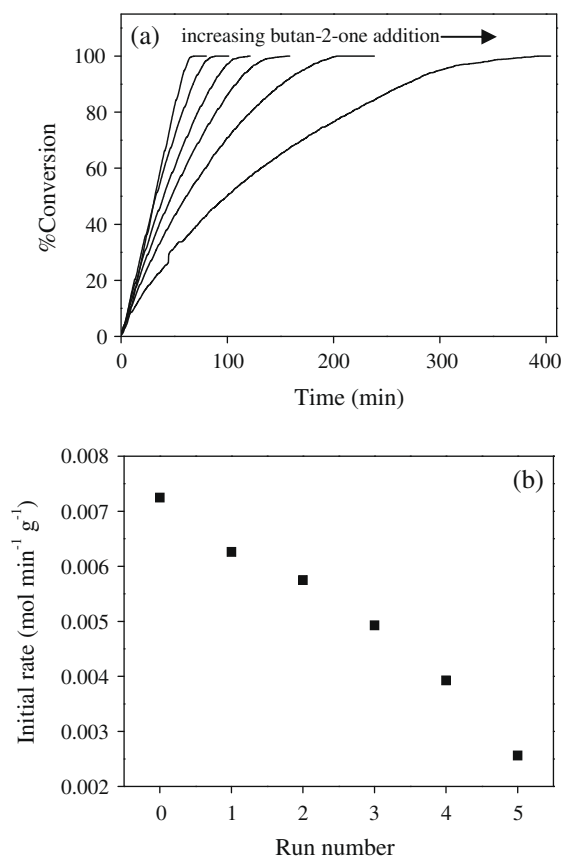
Fig. 2. (a) Butan-2-one conversion with respect to time and (b) the initial hydrogenation rate for sequential experiments without catalyst exposure to air. In each reaction, pure butan-2-one was added to the reaction mixture.
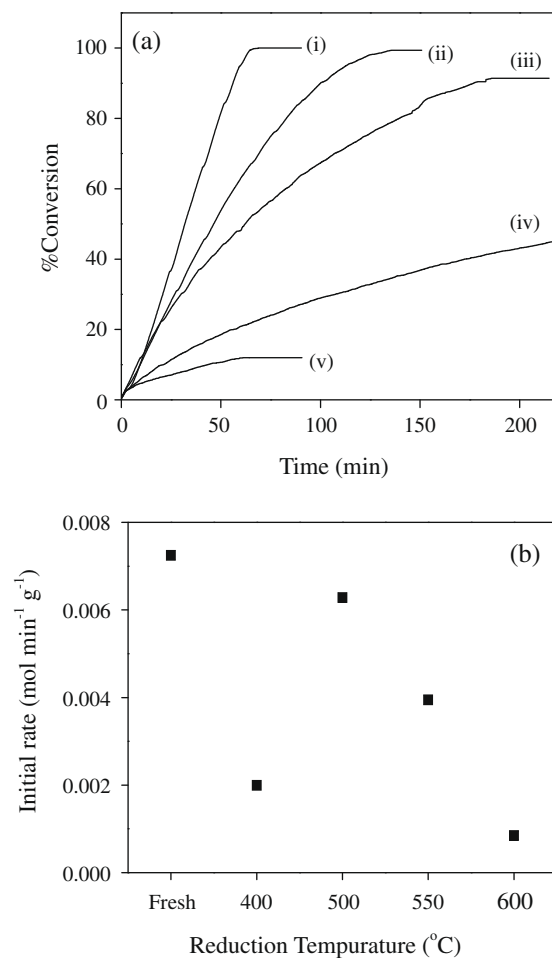

Fig. 3. Comparison of (a) butan-2-one conversion with respect to time for (i) the fresh catalyst and following regeneration of deactivated catalyst by reduction in H$_2$ gas at (ii) 500 °C, (iii) 550 °C, (iv) 400 °C and (v) 600 °C, and (b) the initial hydrogenation rate for the corresponding reactions.

the 1 wt% Ru/SiO$_2$ samples. This indicated that the ruthenium species present on the silica surface were either amorphous or highly dispersed, with particle sizes below the detection limit of the technique, i.e. below approximately 4 nm.

Nitrogen adsorption/desorption analysis at 77 K on the 1 wt% Ru/SiO$_2$ catalyst showed the material to be mainly mesoporous with a total BET surface area of 311 m^2 g^{-1}, mainly from mesopores of characteristic diameters in the range of 11–19 nm with mean pore diameter of 15.1 nm and an average pore volume of 0.95 cm^3 g^{-1}. The high mesoporosity provides facile access to and from the pores for the ketone reagent and alcohol product.
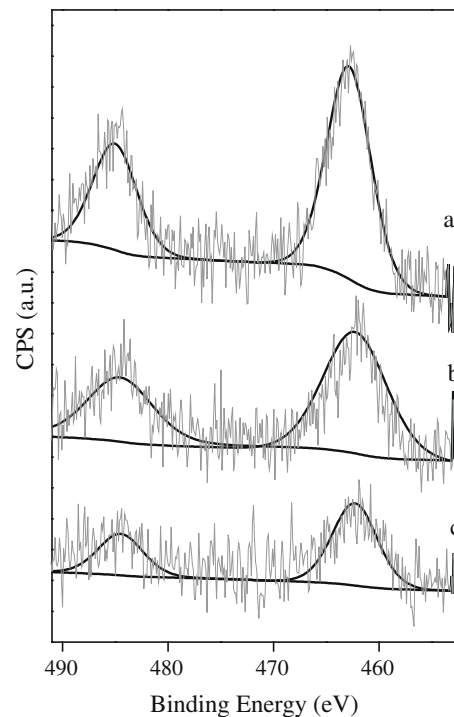
TPR profiles of the fresh, deactivated and regenerated catalysts are shown in Fig. 4. The profile of the fresh catalyst featured a sharp reduction peak with a maximum at ~105 °C, which is attributed to the reduction of RuO$_2$ to Ru(0) [22,23]. In contrast, the profile of the deactivated catalyst showed three reduction peaks centred at ~95, 175 and 330 °C. Reduction peaks at 95 and 175 °C were assigned to the reduction of large and small RuO$_2$ particles, respectively [24]. A comparison of the TPR of Ru(OH)$_3$ prepared by precipitation with the deactivated catalyst indicates that the reduction peak at ~330 °C may be due to the reduction of surface hydroxide species. Fig. 4 also shows the TPR profiles of the catalyst samples regenerated by reduction in the flow of H$_2$ at 400, 500 and 600 °C. TPR profiles of the regenerated catalyst samples showed a broad feature centred between 410 and
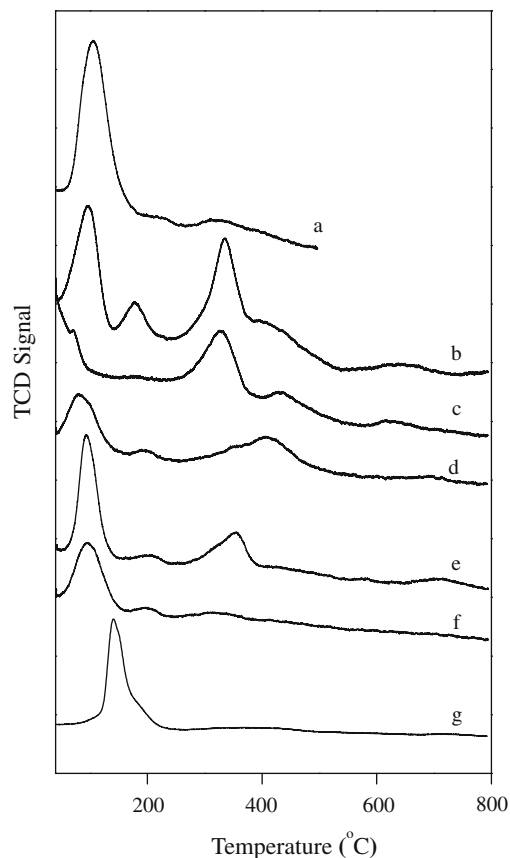
Fig. 4. Temperature-programmed reduction profiles of the fresh, deactivated and regenerated 1 wt% Ru/SiO$_2$ catalysts and 1 wt% Ru(OH)$_3$/SiO$_2$. (a) Fresh, (b) deactivated, (c) Ru(OH)$_3$ + SiO$_2$, (d) regenerated at 400 °C, (e) regenerated at 500 °C, (f) regenerated at 600 °C and (g) heated under Ar at 600 °C.

Fig. 5. XPS spectra of Ru/SiO$_2$ catalyst for Ru 3p spectral lines; (a) fresh, (b) catalyst recovered after reaction and (c) deactivated (hydrated for 6 h).

430 °C. This is thought to be due to the reduction of ruthenium interacting strongly with the silica support [25,26].

CO chemisorption was carried out over the fresh, once used and completely deactivated catalyst samples as well as over the deactivated catalyst samples that were regenerated in the flow of H$_2$ at 500 and 600 °C. The CO uptake for each catalyst is summarized in Table 1. High CO uptake was found for the fresh catalyst indicating a high dispersion of Ru; however, following reaction the CO uptake decreased significantly. Even after high temperature reduction to regenerate the catalyst, the CO chemisorption remained much lower than for the fresh catalyst. From the TPR results it is clear that other ruthenium species are present after reaction, for example a hydroxide, which is likely to contribute to the low CO uptake after reaction. However, the fact that, even after the reduction of these species, a small CO/Ru ratio remains indicates that other non-reducible species remain on the surface of the catalyst which blocks the CO chemisorption [27]. TEM results of the fresh catalyst, the catalyst following reaction in water and the catalyst regener-

ated at 500 °C showed no significant change in the metal dispersion, indicating that at these temperatures no significant sintering of the catalyst had occurred. Low CO uptake for the fresh 1 wt% Ru/SiO$_2$ catalyst that had been pretreated under argon atmosphere at 600 °C for 1 h was also noted; however, TPR analysis of the catalyst heated under argon did not show any surface ruthenium hydroxide species, showing that the surface reaction between Ru and surface silanol groups is unlikely to be the cause of the reduced chemisorption ability (Fig. 4). At these temperatures, sintering is likely explaining the low CO adsorption.

XPS analysis was performed on a fresh catalyst, catalyst recovered after reaction, and deactivated (hydrated for 6 h) samples of 1 wt% Ru/SiO$_2$ catalyst, and the spectra obtained are shown in Fig. 5. The Ru 3p$_{3/2}$ binding energy for the fresh catalyst was observed at 462.8 eV, which is in accordance to the reported values for RuO$_2$ [28]. The Ru 3p binding energies were found to shift to a lower binding energy by 0.5 eV to 462.3 eV for the catalyst recovered after reaction and for that deactivated via hydration for 6 h which is consistent with the formation of surface hydroxide. In addition, the Ru 3p peak areas were found to decrease which may also be associated with the formation of the hydroxide layer.

The catalyst characterization provides some insight into the state of the catalyst following reaction and processes which occur

Table 1
Total CO uptake on 1 wt% Ru/SiO$_2$ during CO pulse chemisorption.

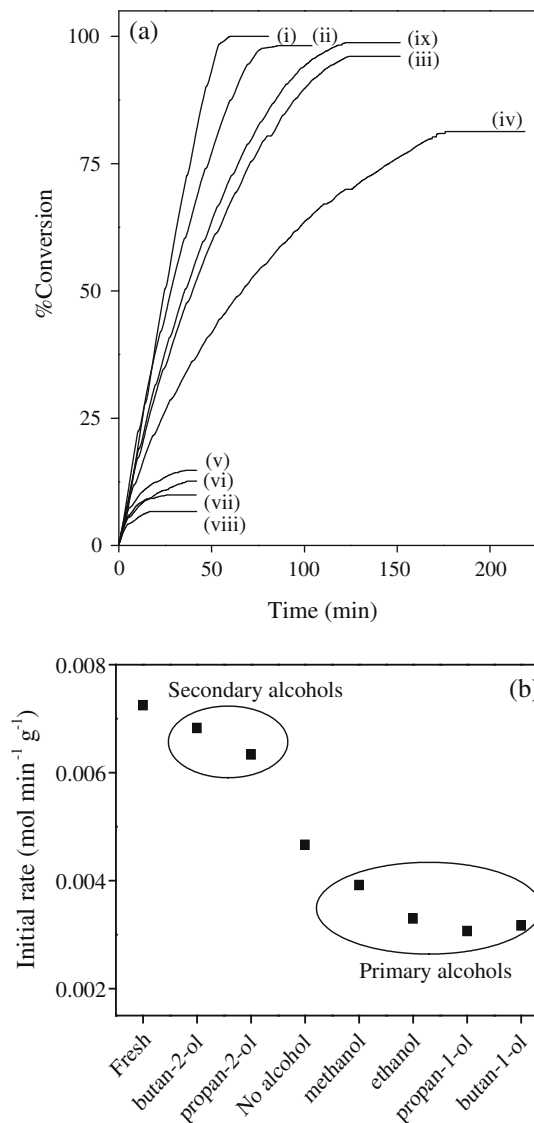| Catalyst	Reduction temperature (°C)	CO/Ru molar ratio
Fresh	500	0.33
Following reaction	500	0.12
Completely deactivated	500	0.01
Regenerated	500	0.03
Regenerated	600	0.02
Heated under Ar atmosphere	600	0.02
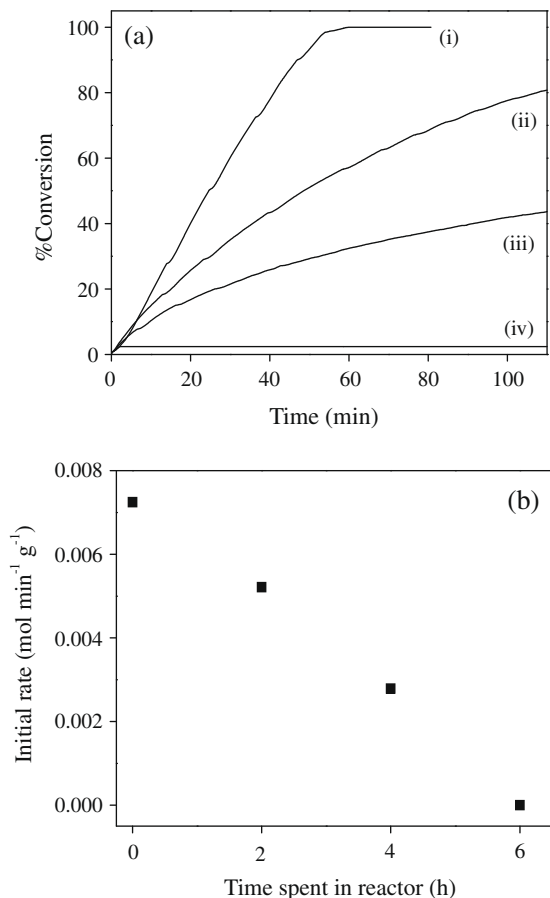
Fig. 6. Comparison of (a) butan-2-one conversion with respect to time for (i) the fresh catalyst and following treatment of the catalyst in water for (ii) 2, (iii) 4 and (iv) 6 h, and (b) the initial hydrogenation rate for the corresponding reactions.

Fig. 7. Comparison of (a) butan-2-one conversion with respect to time and (b) the initial hydrogenation rate of (i) the fresh 1 wt% Ru/SiO$_2$ catalyst with the catalyst following treatment in water–alcohol mixtures using (ii) butan-2-ol, (iii) propan-2-ol, (iv) no alcohol, (v) methanol, (vi) ethanol, (vii) propan-1-ol and (viii) butan-1-ol as well as with (ix) the catalyst washed with butan-2-ol.

during regeneration. From the TPR analysis, complete reduction of Ru(OH)$_3$ requires temperatures >400 °C, consequently the activity for the catalyst regenerated at 500 °C is greater than that regenerated at 400 °C. Although only a small change is observed, the decrease in CO chemisorption ability of the catalyst after treatment at 600 °C compared with treatment at 500 °C may be the reason for the decrease in the activity of the catalyst following regeneration at temperatures >500 °C. In this case, sintering of the ruthenium particles may also occur hence reducing the active surface area as shown from the results of the treatment of the catalyst under Ar at 600 °C [29].

From the catalyst characterization, it is likely that the deactivation during reaction observed both on the recycle of the catalyst and for sequential reactions is due to the formation of Ru(OH)$_x$ on the catalyst surface. In order to examine this formation in more detail a series of experiments were performed where the catalyst was treated in water under typical experimental conditions in the absence of butan-2-one as a function of time in the reactor. Following this pre-treatment, the butan-2-one hydrogenation was performed. Fig. 6 shows variation in reaction profile and initial rate of butan-2-one hydrogenation as a function of the pre-treatment time. A significant decrease in the rate is found as the pre-treatment time was increased with the catalyst treated for 6 h in water showing no significant hydrogenation activity.

3.4. Catalyst deactivation in different water–alcohol mixtures

A series of experiments were also performed in which the catalyst pretreatment was carried out in water–alcohol mixtures for

2 h and the butan-2-one was subsequently added and hydrogenated. A range of primary and secondary alcohols were used namely methanol, ethanol, propan-1-ol, butan-1-ol, propan-2-ol and butan-2-ol. In each water–alcohol mixture, a molar equivalent of alcohol to the butan-2-one normally used in the reaction was added to the water-phase as well as an examination of the effect of butan-1-ol concentration between 0.25 and 1.50 molar equivalents. The reaction profile of the hydrogenation and the initial rate of reaction following each pre-treatment at 1 molar equivalent are shown in Fig. 7. The hydrogenation activity of the catalyst treated in the alcohol-water mixture was significantly influenced by the presence and type of alcohol used. The catalyst treated using both secondary alcohols showed a significantly reduced level of deactivation compared with the catalyst treated in pure water with the deactivation effect more pronounced using the more hydrophobic system, i.e. butan-2-ol < propan-2-ol. In contrast, primary alcohols increased the deactivation of the catalyst compared with treatment with water only. No effect of the alcohol concentration was observed indicating the strong adsorp-
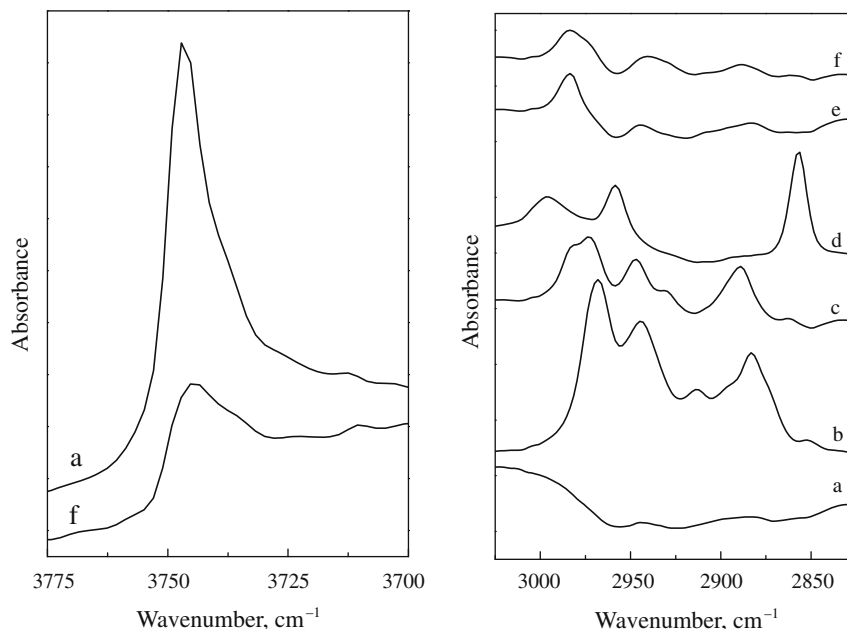
Fig. 8. FTIR spectra of (a) fresh catalyst without pretreatment with alcohol and catalyst treated with (b) butan-1-ol, (c) propan-1-ol, (d) methanol, (e) propan-2-ol and (f) butan-2-ol; ν_{OH} region (3500–3750 cm^{-1}) and δ (COH) region (2850–3000 cm^{-1}).

tion of the alcohol compared with that of the water under these conditions, in agreement with the relative rates of displacement described below.

FTIR spectra of various primary and secondary alcohols physisorbed on fresh 1 wt% Ru/SiO$_2$ catalyst are shown in Fig. 8. The absorption band at ~3745 cm^{-1} is assigned to germinal and isolated Si–OH stretching vibrations. The absorption bands at *ca.* 2800–3000 cm^{-1} correspond to C–H stretching vibrations of physisorbed alkoxyl groups [30–35]. In comparison with the fresh 1 wt% Ru/SiO$_2$ catalyst sample (trace *a*), a significant decrease in the intensity of the Si–OH band was observed for all alcohol-treated samples as illustrated by the spectrum following butan-2-ol adsorption (trace *f*). Quantification of the isolated silanol groups using silylation with TMES shows a decrease from the pure SiO$_2$ (0.40 TMES nm^{-2}) to the fresh 1 wt% Ru/SiO$_2$ (0.25 TMES nm^{-2}) due to blocking of the silica sites on metal deposition. A further decrease is observed following deactivation of the 1 wt% Ru/SiO$_2$ catalyst in water (0.14 TMES nm^{-2}). The decrease in the measured silanol bands following water treatment may be indicative of strongly hydrogen-bonded surface water, which prevents silylation of the silanol groups. This is consistent with DRIFTS spectra of the silylated catalysts before and after water treatment, which showed the presence of significant features associated with surface water.

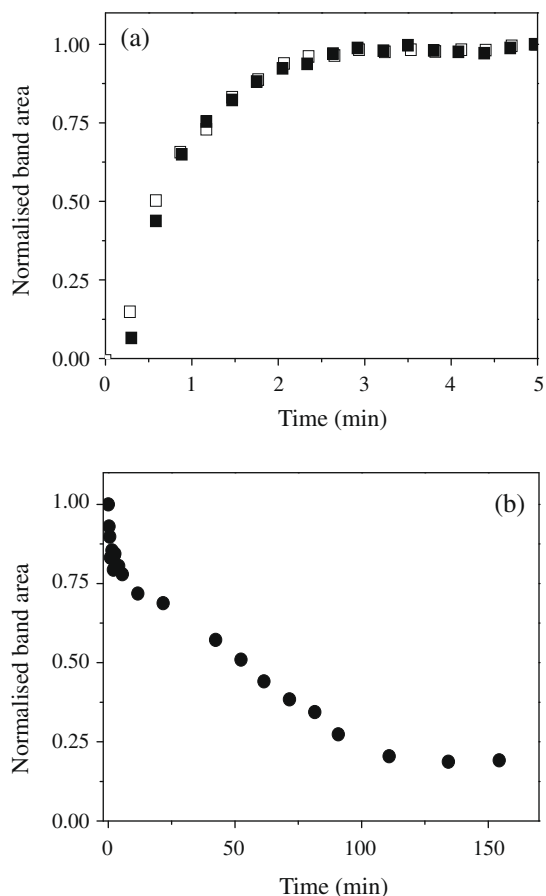Table 2 summarizes the normalized peak areas following the adsorption of each of the alcohols examined. This was accompanied by the appearance of surface alkoxyl group bands, suggesting that the alcohol molecules were adsorbed on the silica surface by reacting with the surface Si–OH groups and, from the silylation data, free silanols are still present even following treatment in water. This is consistent with reports that show that the interaction of alcohols with a silica surface results in decreased density of surface Si–OH groups and an increased surface hydrophobicity [28–30].

The infrared data clearly demonstrate that both the alcohols and butan-2-one adsorb on the silica support with a perturbation of the isolated SiOH band at 3745 cm^{-1} observed. It is also likely that the alcohols adsorb on the ruthenium metal; however, due to the much lower surface area of the metal compared with the oxide little change is observed in the DRIFTS data in the OH stretching region or in the region of Ru–O vibrations (~550–600 cm^{-1}) or Ru–O–C of alkoxy species (~1100 cm^{-1}) [31] or in the carbon monoxide adsorption region (1800–2060 cm^{-1}). Strong adsorption of alcohols on platinum group metals has been observed previously from aqueous solutions and in the gas-phase and results in the formation of alkoxy species as well as C–C bond cleavage products including CO [36].

The increased hydrophobicity of the surface is likely to reduce the water concentration at the surface of the catalyst thereby decreasing the rate of ruthenium hydroxide formation, as shown in Scheme 1. In order to examine the ability of the alcohols to protect the ruthenium from hydroxylation, fresh 1 wt% Ru/SiO$_2$ catalyst was washed with butan-2-ol and the excess of butan-2-ol removed. This treated catalyst was hydrated in water under experimental conditions similar to those used for the hydrogenation reaction in the absence of butan-2-one for 2 h. The activity of the catalyst treated sequentially with alcohol and then water is compared with that of the catalyst treated in pure water in Fig. 7, curves 9 and 4, respectively. Significantly higher activity is found, i.e. less deactivation, for the butan-2-ol-washed catalyst compared with the catalyst washed with pure water, showing that the alcohol can provide a protective coating for the ruthenium to prevent hydroxide formation. The increased hydrophobicity of the butan-2-ol compared with propan-2-ol is reflected by the relative amounts of deactivation observed.

Table 2
Comparison of normalized peak areas for absorption band at 3745 cm^{-1}, assigned to Si–OH stretching vibrations from FTIR spectra of catalyst pretreated with different alcohols.

| Alcohol	Normalized peak area
Fresh catalyst (w/o pretreatment)	1
Butan-1-ol	0.524
Propan-1-ol	0.617
Methanol	0.629
Propan-2-ol	0.695
Butan-2-ol	0.256

Fig. 9. Change in normalized C–H stretching band areas of propan-2-ol with time for (a) propan-2-ol adsorption on the fresh catalyst and on a water-saturated surface and (b) propan-2-ol desorption in the presence of a water atmosphere. The normalized band areas at different times are represented by the symbols (□) propan-2-ol adsorption on a fresh catalyst, (■) propan-2-ol adsorption on a water-saturated surface and (•) propan-2-ol desorption by the presence of water.
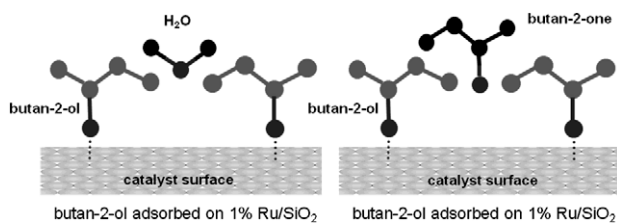
Scheme 1. Schematic illustrating the effect of butan-2-ol adsorption on 1 wt% Ru/SiO_2 catalyst for the interaction of water with the catalyst surface.

The increased hydrophobicity of the catalyst surface following interaction with the secondary alcohols is supported by a DRIFTS examination of the adsorption of water and propan-2-ol and by an assessment of the relative rate at which these adsorbed species can displace each other from a 1 wt% Ru/SiO_2 catalyst surface. Fig. 9 shows that the rate of propan-2-ol build up on the reduced surface is comparable to that found on the water saturated Ru/SiO_2 surface with the surface becoming saturated with propan-2-ol within 5 min of switching the feed with, in both cases, comparable intensities of the bands observed after 5 min. However, when propan-2-ol was preadsorbed on the surface and the feed switched to water, the displacement of the surface species was significantly slower taking tens of minutes. This indicates that the propan-2-ol can effectively block water adsorption as indicated by the proposed
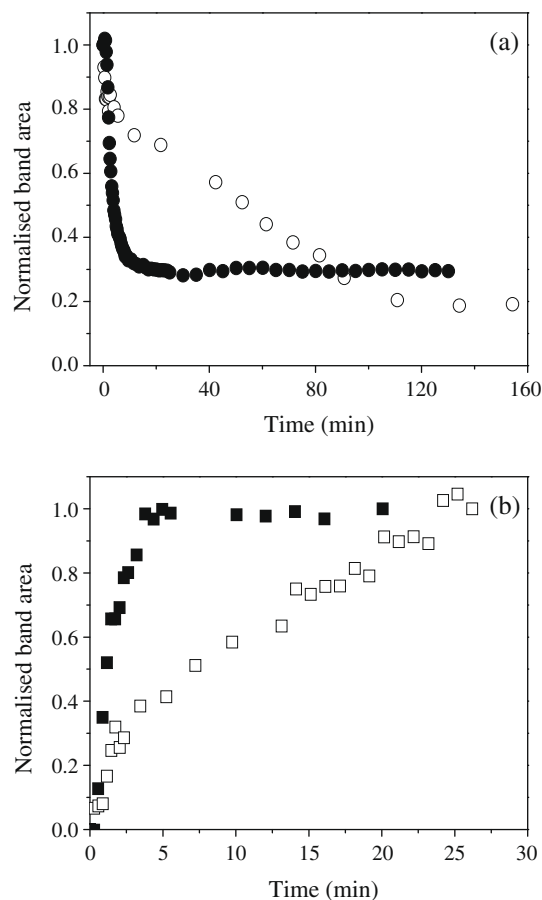

Fig. 10. Comparison of the change in normalized C–H stretching band areas of propan-2-ol and propan-1-ol with time for (a) water displacing propan-1-ol (○) or propan-2-ol (•) and (b) (■) butan-2-one displacing propan-2-ol and (□) butan-2-one displacing propan-1-ol from the catalyst surface.

reaction mechanism. Interestingly, although the propan-2-ol has a significant effect on the adsorption of water, the effect on butan-2-one adsorption is limited with the butan-2-one and propan-2-ol displacing each other at comparable rates (Fig. 10). The effect of the secondary alcohol on water adsorption may be compared with the results following preadsorption of propan-1-ol on the surface of the catalyst. In this case, water displaces the primary alcohol rapidly compared with propan-2-ol, as shown in Fig. 10. Despite this rapid initial displacement, there is a residual amount of propan-1-ol remaining on the surface which cannot be removed even after 120 min of exposure to water vapour. It is possible that the remaining propan-1-ol is localized around the metal sites and similarly to propan-2-ol controls access of the water and, possibly, butan-2-one to the catalyst surface.

The significantly lower hydrogenation activity of catalysts treated with primary alcohols may be explained by considering the orientation of surface-adsorbed alkyl chains. In the case of the secondary alcohols, the hydrocarbon chains align parallel to the catalyst surface leading to a low packing efficiency. Whilst this increases the hydrophobicity of the surface it does not prevent water, necessary for the proton shuttle mechanism outlined earlier, from interacting completely and also allows the polar carbonyl group of the butan-2-one to interact with the active sites (Scheme 1). In the case of primary alcohols, the alkoxy species adsorb perpendicular to the surface. Through strong van der Waals interactions, the hydrocarbon chains align with each other, and a high density of hydrocarbon is possible (Scheme 2). This increased packing of alcohol molecules allows the surface to become significantly more
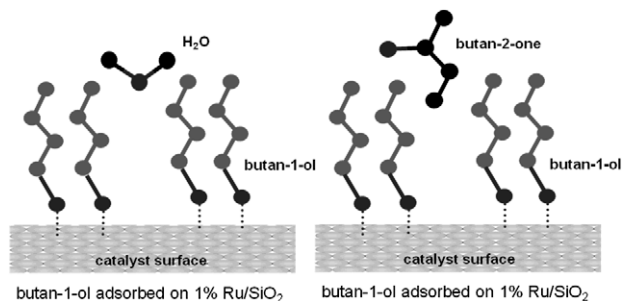
Scheme 2. Schematic illustrating the effect of butan-1-ol adsorption on 1% Ru/SiO$_2$ catalyst for the interaction of butan-2-one and water with the catalyst surface.

hydrophobic than for the case of the secondary alcohols. As the chain length is increased this effect is exacerbated and the water concentration at the surface diminishes significantly, which is consistent with the rates of reaction given in Fig. 7, where the deactivation for butanol > propan-1-ol > ethanol > methanol. Whilst this results in less hydration, potentially, the low energy hydrogenation pathway is switched off resulting in a highly deactivated catalyst.

4. Conclusions

One weight percentage of Ru/SiO$_2$ catalyst showed excellent hydrogenation activity in the liquid-phase hydrogenation of butan-2-one in water as a solvent. The catalyst also showed good reusability with complete conversion in each subsequent recycle; however, the initial hydrogenation rates exhibited a decreasing trend in each subsequent run due to gradual catalyst deactivation. TPR, CO adsorption and XPS analyses showed that the deactivation was consistent with the formation of surface hydroxide. Regeneration conditions for the completely deactivated catalyst were optimized and up to 85% of the initial activity can be successfully regained. It was observed that the presence of secondary alcohols in the reaction medium protected the Ru/SiO$_2$ catalyst from deactivation, whereas significant deactivation was found in the case of primary alcohols. Both primary and secondary alcohols may form a hydrophobic layer around the active metal; however, through a combination of steric effects and adsorption geometry, only the secondary alcohol allows sufficient interaction of the water and butan-2-one with the catalyst to allow significant hydrogenation activity to be maintained.

Acknowledgments

References

[1] C.H. Bartholomew, Appl. Catal. A 107 (1993) 1.
[2] C.H. Bartholomew, Appl. Catal. A 212 (2001) 17.
[3] P. Albers, J. Pietsch, S.F. Parker, J. Mol. Catal. A 173 (2001) 275.
[4] J.A. Moulijn, A.E. van Diepen, F. Kapteijn, Appl. Catal. A 212 (2001) 3.
[5] L.-P. Tiainen, P. Mäki-Arvela, A.K. Neyestanaki, T. Salmi, D.Y. Murzin, React. Kinet. Catal. Lett. 78 (2) (2003) 251.
[6] R. Hughes, Deactivation of Catalysts, Academic Press, New York, 1984.
[7] L. Petrov, K. Kumbilieva, J. Univ. Chem. Tech. Metall. 41 (1) (2006) 5.
[8] M. Besson, P. Gallezot, Catal. Today 81 (2003) 547.
[9] B. Arena, Appl. Catal. A 87 (1992) 219.
[10] K. Petr, C. Libor, Appl. Catal. A 229 (1–2) (2002) 193.
[11] R.-V. Virginie, G. Jean-Pierre, J. Organomet. Chem. 567 (1–2) (1998) 163.
[12] P. Kluson, L. Cerveny, Appl. Catal. A 128 (1995) 13.
[13] P.D. Vaidya, V.V. Mahajani, Chem. Eng. Sci. 60 (2005) 1881.
[14] G. Held, J. Weissenrieder, A. Mikkelsen, J.N. Andersen, P.J. Feibelman, Phy. Rev. Lett. 93 (19) (2004) 196102.
[15] P.N. Rylander, in: W.H. Jones (Ed.), Catalysis in Organic Synthesis, Academic Press, New York, 1980.
[16] S.K. Desai, M. Neurock, Phys. Rev. B 68 (2003) 075420.
[17] B. Hu, R.P. Fishwick, A.W. Pacek, J.M. Winterbottom, J. Wood, E.H. Stitt, A.W. Nienow, Chem. Eng. Sci. 62 (2007) 5392.
[18] K. Hindle, D.W. Rooney, B.S. Akpa, L.F. Gladden, D. Weber, M. Neurock, N. Sinha, E.H. Stitt, in: 19th International Symposium on Chemical Reaction Engineering, Potsdam, Germany, 2006.
[19] S.L. Hruby, B.H. Shanks, J. Catal 263 (2009) 181.
[20] R.R. Sever, R. Alcala, J.A. Dumesic, T.W. Root, Micropor. Mesopor. Mater. 66 (2003) 53.
[21] D.A. Shirley, Phys. Rev. B 5 (1972) 4709.
[22] P. Betacourt, A. Rives, R. Hubaut, C.E. Scott, J. Goldwasser, Appl. Catal. A 170 (1998) 307.
[23] S.-C. Hu, Y.-W. Chen, Ind. Eng. Chem. Res. 40 (2001) 6099.
[24] F. Orellana, J. Plaza de los Reyes, S. y Urizar, J. Chil. Chem. Soc. 48 (2) (2003) 33.
[25] J.W. da-Silva, A.J.G. Cobo, Appl. Catal. A 252 (2003) 9.
[26] P. Reyes, M.E. Konig, G. Pecchi, I. Concha, M.L. Granados, J.L.G. Fierro, Catal. Lett. 46 (1997) 71.
[27] G.H. Yokomizo, C. Louis, A.T. Bell, J. Catal. 120 (1989) 1.
[28] D.D. Sarma, C.N.R. Rao, J. Electron Spectrosc. Relat. Phenom. 20 (1980) 25.
[29] Z. Opre, J.-D. Grunwaldt, M. Maciejewski, D. Ferri, T. Mallat, A. Baiker, J. Catal. 230 (2) (2005) 406.
[30] D. Jiang, Y. Ding, Z. Pan, W. Chen, H. Luo, Catal. Lett. 121 (2008) 241.
[31] S.-L. Guo, M. Arai, Y. Nishiyama, Appl. Catal. 65 (1) (1990) 31.
[32] C.J. Brinker, G.W. Sherer, Sol–Gel Science, Academic Press, London, 1990.
[33] J.P. Camplin, E.M. McCash, J. Chem. Soc. Faraday Trans. 92 (1996) 4695.
[34] Q.H. Xia, K. Hidajat, S. Kawa, Catal. Today 68 (2001) 255.
[35] J.H. Zimnoch dos Santos, P.P. Greco, F.C. Stedile, J. Dupont, J. Mol. Catal. A Chem. 154 (2000) 113.
[36] P. Gao, C.H. Lin, C. Shannon, G.N. Salaita, J.H. White, S.A. Chaffins, A.T. Hubbard, Langmuir 7 (7) (1991) 1515.